Chinese Chemical Letters 32 (2021) 2923–2932

Contents lists available at ScienceDirect

Chinese Chemical Letters

journal homepage: www.elsevier.com/locate/cclet

Review

3D printing hydrogels for actuators: A review

Aokai Zhang[a,1], Feng Wang[b,1], Lian Chen[b], Xianshuo Wei[b], Maoquan Xue[a], Feng Yang[a,*], Shaohua Jiang[b,*]

[a] Changzhou Institute of Industry Technology, Changzhou 213164, China
[b] Co-Innovation Center of Efficient Processing and Utilization of Forest Resources, College of Materials Science and Engineering, Nanjing Forestry University, Nanjing 210037, China

ARTICLE INFO

Article history:
Received 20 February 2021
Received in revised form 19 March 2021
Accepted 28 March 2021
Available online 30 March 2021

Keywords:
Soft robotics
Hydrogel
3D printing
Biomaterials
Actuator
Finite element analysis

ABSTRACT

Soft and wet actuator systems have attracted great attention in some applications, such as assistive technologies for rehabilitation, training and regenerative biomedicines. Three-dimensional (3D) printing methods have realized the rapid fabrication of complex structures without the need for expensive dies or post processing. In this review, a comprehensive description is presented on stimuli-responsive hydrogels fabricated by light-responsive and extrusion-based 3D printing technologies. Mechanisms of actuations have been introduced based on stimuli types. As the most common method for 3D printed hydrogel actuators, direct-ink-writing has been discussed, including the two printing parameters of resolution and rheology. In addition, applications of 3D printed hydrogel actuators are presented followed by introductions of recent contributions on enhancing the toughness of 3D printed hydrogel and robust design tools, such as finite element analysis and artificial intelligence.

1. Introduction

Actuators refer to parts of robots or machines that are responsible for the movements [1–4]. Traditional actuators are typically planar and brittle, rendering themselves incompatible with human-machine interfaces or biological environment. Hydrogels are networks consisting of polymer chains [5–10]. They usually contain more than 90 wt% of water, while still retain its integrity and strength for use of structural materials [10–14]. Owing to their high water-content, hydrogels possess high biocompatibility which render them good choices for biomaterials for bone regeneration [15,16], wound healing [17–19], self-healing [20,21], drug delivery [22,23] and cell culture [24–27]. High biocompatibility makes hydrogels promising materials for soft actuators, which calls for more and more interactions between human and robots [28,29].

Hydrogels show large volume changes in response to a large range of stimuli including light [30], temperature [31,32], pH [33,34], salt [35], biomolecules [36], electric [37,38] and magnetic field [39]. To get actuation movements, it needs either a homogeneous hydrogel structure with anisotropic stimuli [40] or an anisotropic structure with homogeneous stimuli [41,42]. The latter is more commonly used because it is more convenient to generate isotropic stimuli. The anisotropic hydrogel structures can be prepared from patterning techniques such as ion inject printing [43] and sacrificial printing [44], while 3D printing, also known as additive manufacturing, offers rapid design and powerful fabrication of complex 3D structures [45,46]. A number of comprehensive reviews has covered the areas of hydrogel actuators [47,48] as well as the 3D printable soft matter [2,9,49,50]. However, to the best of our knowledge, there are still countable reports on summarizing the development on the 3D printable hydrogel actuators.

Therefore, in this review article, the progress and development on the 3D printable hydrogel actuators are summarized (Scheme 1). First of all, problems of address or requirements of product should be defined, at the same time, the necessity of using 3D printing hydrogels will be discussed. When looking into the details of the fabrication, careful considerations are needed to be taken based on the balance among the design of materials, printing methods, and actuation. The choice of materials may be function-oriented. The response to different stimuli, a kind of physico-chemical properties, are usually determined by the chemical- and micro- structures of the hydrogels. In addition, fabrication methods also deserve attentive attention as different synthesis tools renders diverse hydrogel network structures and distinct properties. As for the printing process, specific 3D printing

* Corresponding authors.
E-mail addresses: yangfeng@ciit.edu.cn (F. Yang), shaohua.jiang@njfu.edu.cn (S. Jiang).
[1] These two authors contributed equally to this work.

https://doi.org/10.1016/j.cclet.2021.03.073
1001-8417/

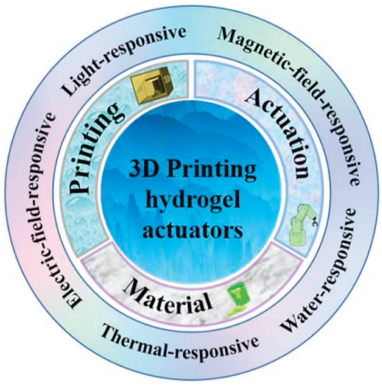

Scheme 1. Summary of 3D printed hydrogel actuators.

technique will be determined by the material characteristics and product properties. Depending on the formation mechanisms, 3D printings can be divided into light-curing 3D printing and direct ink writing (DIW), which are the most frequently used for producing hydrogels and will be discussed intensively below. Printing parameter such as printing velocity, temperature and pressure can be generally changed based on the materials used. When it comes to the fabrication process, digital 3D structures will be transferred to cross-sectional data like computed tomography for printing. In this period, printing parameters will be refined and adjusted to achieve desirable condition. As for the actuation and applications, soft actuators can either be integrated in soft robots or undergo unit test to obtain its actuation or mechanical properties. Material design and printing parameters can be optimized to achieve superior properties such as faster actuation time and higher printing resolution, depending on the raw materials and the products. Furthermore, tools such as finite element analysis [51] and artificial intelligence [52] can provide insights into the optimizations of materials, structures and printing parameters.

In this review, recent advances in 3D printed hydrogel actuators will be summarized with an emphasis on actuation mechanism. In addition, the application of the materials will be introduced followed by a glance on the design criteria such as methods to improve actuation time and printing resolution, to enhance toughness, and to accelerate fabrication and design. The authors hope this contribution can serve as a connection for scientists and engineers in the fields of 3D printing, hydrogels and actuators.

2. Light-curing 3D printing for hydrogel actuators

2.1. Stereo lithography (SLA)

Stereo lithography (SLA) is one of the most mature 3D printing techniques. In SLA, the fluid ink is printed layer by layer. At the same time, the surface is irradiated by laser to solidify the chosen area. This process continues until the required product is obtained.

Ion responsive hydrogel actuators are usually realized by employing a multi-material structure consisting of ion-responsive gel (polyelectrolyte) and neutral non-ion-responsive gel layers. Mismatched contraction of two layers could control bending and twisting actuation. For example, Wong and colleagues have fabricated bi-material hydrogel actuators by SLA of neutral poly (ethylene glycol) diacrylate at the presence of anionic poly(acrylic acid) [53]. UV light was used to crosslink poly(ethylene glycol). Fe^{3+} was used as an ionic crosslinker of the anionic carboxyl groups associated with poly(acrylic acid). Thus the bi-layer hydrogels underwent large volume change in response to external ion concentration, showing bend actuation behavior upon immersion

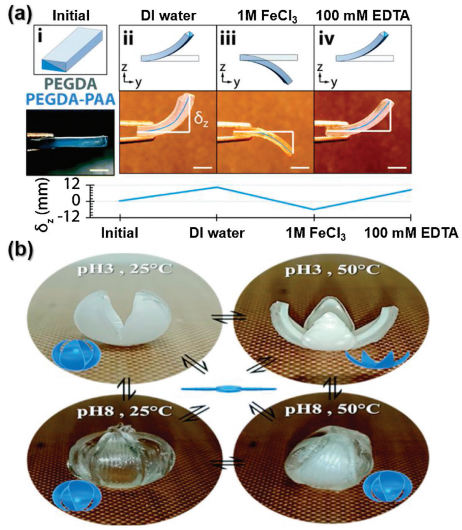

Fig. 1. (a) SLA printed bi-layer cantilever designed for multiplanar twisting simultaneously imaged from the side. Reproduced with permission [53]. Copyright 2019, Royal Society of Chemistry. (b) Temperature and pH dual-responsive actuation of an SLA printed gradient-like structure of varying layer compositions across the hydrogel. Reproduced with permission [54]. Copyright 2019, Royal Society of Chemistry.

in DI water, $FeCl_3$ and EDTA solutions (Fig. 1a). Another advantage of the chemical structure of actuators lied in the formation of ionic crosslinks that bridged between surfaces, which greatly enhanced the self-adhesive properties and enabled its application as "plug-and-play" parts.

The Raquez research group has designed SLA printed hydrogel actuators that respond to temperature, pH and osmotic pressure [54]. Here, volume change at lower critical solution temperature (LCST) of poly(*N*-isopropylacrylamide) (PNIPAm) and at pK_a of poly (2-carboxyethylacrylate) (PCEA) rendered the actuators temperature and pH responsive respectively. High resolution SLA was used to fabricate hydrogels with anisotropic structures consisting of multi-layers of PNIPAm and PCEA. The hydrogels showed temperature and pH dual-responsive actuation (Fig. 1b). By changing swelling ratios, crosslinking density and chemical composition of discrete layers, the authors have successfully obtained well control of anisotropic swelling properties, thus achieving precise predict of the folding movement. This work provided a flexible platform for designing advanced actuators with precise structures and controlled movements.

With the growing demand in various functions of materials, SLA technique is gaining new developments by combing with other technologies [55]. In order to print two types of hydrogels, Mishra and co-workers employed SLA combined with "vat replacement" strategies for functional graded actuators [56]. The pH responsive and antimicrobial hydrogel scaffolds have been fabricated based on polyethylene glycol dimethacrylate and acrylic acid, indicating potential of applying SLA printed hydrogel in tissue engineering [57].

2.2. Multiphoton lithography

Multiphoton lithography (MPL), known as direct laser writing, has been also employed to fabricate hydrogel actuators [58]. For example, a light-driven actuator with programed printing density was printed by MPL technique (Fig. 2). Here, gold nanorods (AuNRs) were incorporated in PNIPAm matrix to convert light energy to heat, consequently induced the volume phase transition of PNIPAm gels. The energy conversion was fast (more than 20 °C within milliseconds), thus may accelerate the actuation of gels.

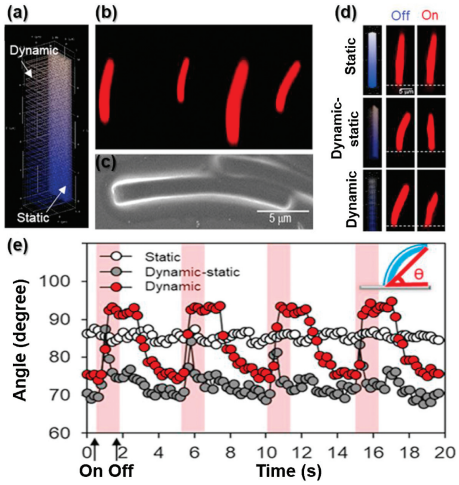

Fig. 2. Actuation of MPL printed bilayer pillar with programmed printing density. (a) CAD image of the bilayer pillar; (b) 3D-reconstructed CLSM image; (c) FESEM image of bilayer pillars; (d) Cross-sectional CLSM images of stiff and soft monolayer pillar and bilayer pillar when the laser was turned on and off; and (e) Angle change of three types of pillars as a function of time when the laser was turned on at 1 Hz and off at 0.2 Hz. Reproduced with permission [59]. Copyright 2020, American Chemical Society.

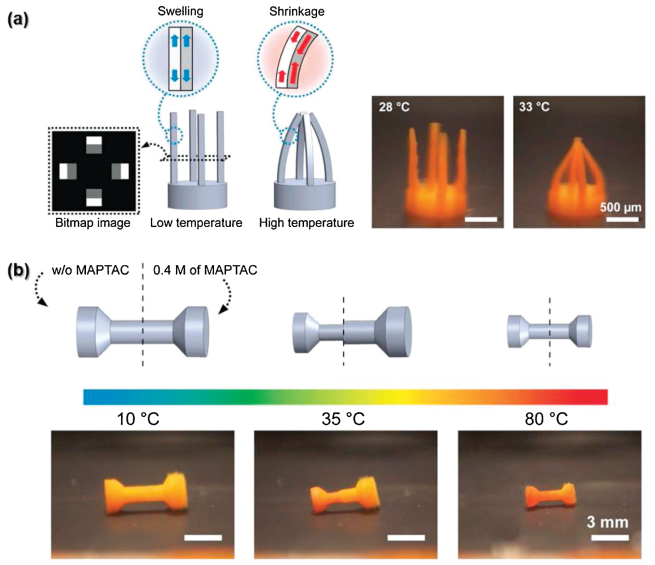

Fig. 3. PμSL printed PNIPAm micro-structures and their programmed temperature dependent deformation. (a) A gripper consisting of four beams was fabricated using two different grayscale levels. The difference in the swelling ratio between the two regions caused the beams to bend towards the center at high temperature (scale bar: 500 μm). (b) A dumbbell-shaped structure was printed with ionic monomer, MAPTAC. The left half is pure PNIPAm while the right half contains 0.4 mol/L of MAPTAC. When temperature increases, the left half with lower transition temperature begins to shrink first, and the right half shrinks later at higher temperature (scale bar: 3 mm). Reproduced with permission [64]. Copyright 2018, Springer Nature.

Furthermore, the authors have investigated the effects of multi-functional macrocrosslinkers in controlling printing density [59].

Employing femtosecond laser direct writing (fsLDW), a point-by-point scanning method, a series of humidity-responsive hydrogel actuators were fabricated. The swelling property could be regulated by changing the crosslinking density of voxels during printing [60]. By choosing appropriate materials, MPL has also been utilized to fabricate hydrogel actuators that response to pH [61], light [62], ion [63], *etc.*

2.3. Projection micro-stereo lithography (PμSL)

Projection micro-stereo lithography (PμSL) is another light-responsive 3D printing method endowed with high resolution. The feature of PμSL lies in that sliced digital image from 3D model is transferred to a digital mask to pattern ultra-violet light, which is then projected through a reduction lens and focused on the surface of the photo-curable material. By PμSL, Lee and colleagues have fabricated temperature-responsive hydrogel micro-structures with high resolution (Fig. 3) [64]. As a demonstration, a gripper consisting of four beams was fabricated using two different levels of grayscale. The difference in light intensity leaded to the swelling anisotropy and result in a precisely controlled thermal actuation of the actuators. They have also employed PμSL to demonstrate soft robotic manipulation and locomotion of high definition 3D printed electroactive hydrogel actuators [65].

Apart from UV laser, a visible safelight has also been utilized to fabricate stimuli-responsive soft actuators [66,67] where the method is always referred as digital light processing (DLP). Employing DLP-based PμSL, the Lee group has presented a novel multi-material system using dynamic fluidic control within an integrated fluidic cell [68]. This method overcame the difficulty of PμSL printing multiple materials that usually required solution exchange in the vat and was a promising tool for rapid fabrication of multi-responsive hydrogel actuators.

3. Direct ink writing (DIW) for hydrogel actuators

Despite the advantage of high resolution, light curing methods are limited to photopolymerizable materials. In contrast, the ink-based methods can obtain complex shapes based on all printable soft materials. The main requirements of printability include viscosity, surface tension and shear yield stress. Among various ink-based techniques, direct ink writing (DIW) may be the most popular 3D printing technique for hydrogel actuators. DIW is a method that raster a syringe with a nozzle across a surface as it dispenses an ink, where the ideal ink is a shear-thinning material [69]. The fabrication temperature is low when compared to other ink-based method such as fused deposition modeling (FDM) that will reach around 200 °C [70]. The mild temperature can prevent the degradation of hydrogel inks and deactivation of bioinks with cells embedded. DIW is also characterized with its high flexibility for multi-material printing to achieve various functions.

3.1. Light-responsive hydrogel actuators by DIW

Light-responsive actuators have the advantage of remote and non-contact control. Graphene oxide (GO), with an extraordinary photo-thermal conversion, has been widely selected as near-infrared light absorbents in actuators [71,72]. When combined with PNIPAm, GO can generate heat under near-infrared light (NIR) and induce the volume transition of PNIPAm [73]. Zhang and co-workers have reported a method to spontaneously align GO flakes in sodium alginate. The hydrogel could be fast actuated into versatile morphology upon light, heat and vapor stimulation [74]. In another case, GO has been dispersed in chitosan (CS) hydrogels, where the heat generated by GO's photothermal effect induced the water gratitude [33]. The hydrogel was fabricated as a light-driven smart curtain responsive to both NIR-light and sunlight (Fig. 4). The actuation speed of GO-dispersed hydrogels was found to highly depend on GO concentration. With a miniaturized prototype actuator based on PAA-GO-Ca^{2+}, the motion velocity was found to increase almost linearly with increasing GO content in the range of 0%–8% [75]. Apart from GO, acrylate groups have been

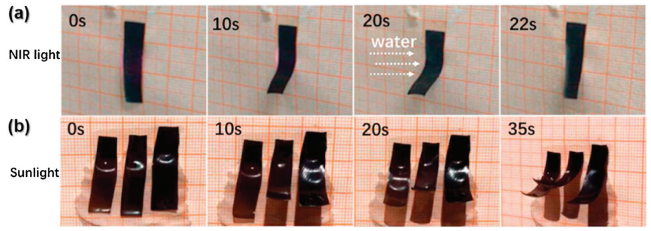

Fig. 4. (a) CS/GO (5%) hydrogel film fabricated as a NIR-light-driven smart curtain. The smart curtain deformation process and recovery induced by water were recorded at different times. (b) CS/GO (5%) hydrogel films fabricated as a sunlight-driven smart curtain. The hydrogel deformation process was recorded at different times by a camera. Reproduced with permission [33]. Copyright 2020, American Chemical Society.

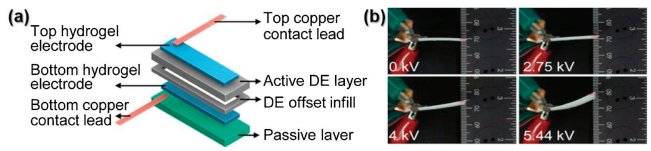

Fig. 5. (a) Schematic of depositing hydrogel on the surface of silicone-based layer treated with BP under UV light exposure. (b) Stills of device actuation performance at different applied voltages. Reproduced with permission [81]. Copyright 2018, Elsevier.

introduced to polyurethane hydrogels to serve as photosensitive moieties for 3D cell-laden bioprinting [76].

3.2. Electric-field-responsive hydrogel actuators by DIW

Polyelectrolyte hydrogels are charged polymer networks with ions fixed on polymer chains [77]. In a series of pioneering works on 3D printed polyelectrolyte hydrogel actuators conducted by Kaynak and co-workers, chitosan was chosen to fabricate the electric-field responsive actuators with contactless electrodes [78–80]. The McAlpine research group has reported the first demonstration of 3D printing ionic hydrogel-elastomers hybrids for electrically responsive actuators (Fig. 5). Here, hydrogel monomer (acrylamide) and silicon were employed in a DIW process, leading to the formation of a silicon-based dielectric elastomer actuators (DEAs) with ionic hydrogel electrodes. The fabricated actuator was able to generate high bending motion in response to electrical stimuli. Also, the integrated ionic hydrogel offered self-sensing capability which resembled the signal transfer mechanism in human skin [81].

3.3. Thermal-responsive hydrogel actuators by DIW

With a rapid and reversible volumetric change at LCST, PNIPAm has been widely employed in fabrication of thermal-responsive hydrogels [82,83]. The volume change of PNIPAm hydrogel might also trigger the variation of conductivity. A 3D printed NIPAm hydrogel actuator with nanoclay and CNT embedded inside was successfully fabricated by Guo and co-workers. The actuator not only responded to heat and near-infrared light rapidly, but also was excellent candidates for pressure-dependent devices to monitor human motions including finger bending, wrist bending, *etc.* [84].

Apart from phase transition of PNIPAm gels, sol-gel transition has also been used to design thermal-responsive hydrogel actuators. For example, by writing agarose/acrylamide/Laponite ink, Zhang, Cao and co-workers have demonstrated a route for 4D printing robust hydrogel that could reversibly soften and harden by temperature. This function was attributed by the sol-gel transformation behavior of agarose. In addition, Laponite, a kind of nanoclay, was found out to endow the ink with shear-thinning behavior and make the ink suitable to print [85].

Another kind of thermal-triggered actuator was demonstrated using a combination of α-cyclodextrin and polyrotaxane (Fig. 6), which has been used for functional materials [86,87]. In this work, Ke and co-workers have constructed methylated compound, where the methylated polyrotaxane exhibited a thermo-responsive sol-gel transition, and the thermo-triggered α-cyclodextrin ring motions contributed to temperature-dependent size change, transparency variation and elastic moduli switching [88].

3.4. Water-responsive hydrogel actuators by DIW

As the most abundant bio-macromolecule in nature, cellulose can respond to water owing to the forming of hydrogen bond of hydroxyl groups. Cellulose-based hydrogels have been fabricated by DIW for potential applications in biomaterials [89]. The Lewis research group has conducted a pioneering work to utilize 3D printed hydrogel in shape morphing. The ink was composed of stiff cellulose fibrils embedded in a soft acrylamide matrix, which mimicked the composition of plant cell walls. The printed bilayer structure could be programmed to change its morphology on immersion in water as time elapsed, which fulfilled the concept of "4D printing" [90]. A series of nanofibrillated cellulose (NFC) – reinforced PDMAA hydrogels has been prepared by Zhou and co-workers. NFC not only provided swelling-induced actuation but also enhanced mechanical properties of the actuators [91]. The readers are referred to several comprehensive reviews on cellulose-based hydrogel for biomedical applications taking advantage of its single or multi responsiveness [92,93].

Lu and co-workers have fabricated a 3D printable ink based on natural egg white (EW) (Fig. 7). Based on swelling ratio mismatch of original EW hydrogel and Fe^{3+} crosslinked one, a humidity-responsive actuator was developed by coating $FeCl_3$ on the hydrogel surface. The ion penetration process created gradient crosslink density, which leaded to a swelling gradient and thus the bending of the hydrogel film [94].

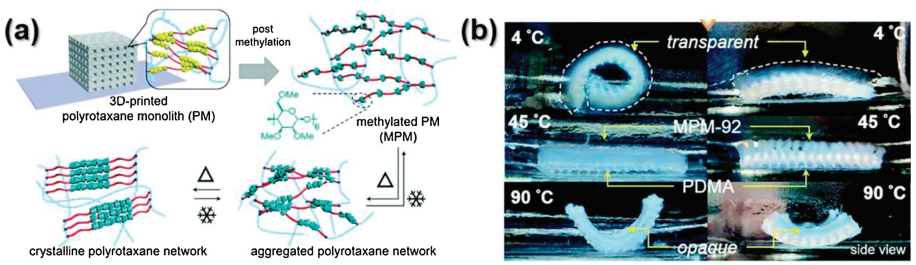

Fig. 6. (a) Illustration of the post 3D-printing methylation of a polyrotaxane monolith, and the molecular level α-CD ring transitions in the thermally responsive methylated α-CD-based polyrotaxane monoliths at different temperatures; and (b) temperature-induced shape morphing of two bilayer monoliths. Reproduced with permission [88]. Copyright 2020, Royal Society of Chemistry.

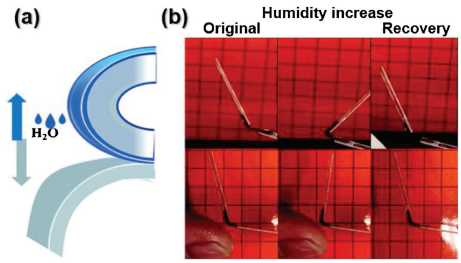

Fig. 7. (a) Schematic of the gradient tailored humidity-responsive EW actuator. (b) The film could bend/unbend repetitively by changing the ambient humidity and was sensitive to an approaching finger. Reproduced with permission [94]. Copyright 2019, Royal Society of Chemistry.

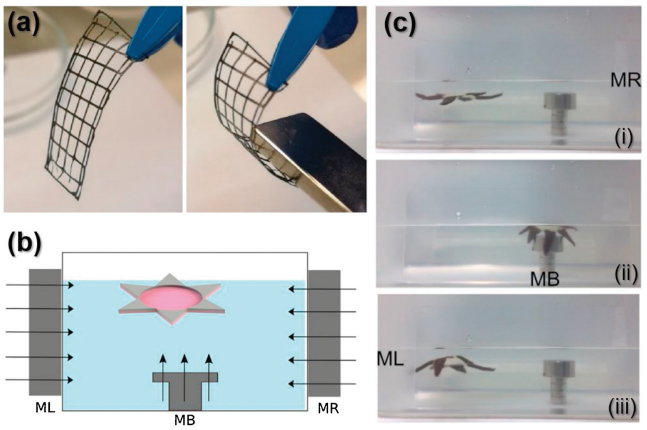

Fig. 8. (a) The magnetic responsivity of the hydrogel to the neodymium magnet a thin hydrogel tile that can be bent, folded and attracted to the neodymium magnet. Reproduced with permission [95]. Copyright 2020, Elsevier. (b) Schematic representation of remote control of the soft robot motion through on/off switching of three electromagnets. (c) Digital image sequence of the starfish robot in (i-iii) swimming and (ii) wrapping motion. Reproduced with permission [97]. Copyright 2018 Wiley-VCH.

3.5. Magnetic-field-responsive hydrogel actuators by DIW

Magnetic-field responsive hydrogel actuators could be prepared from hydrophilic monomers crosslinked in a dispersion of magnetic nanoparticles (MNPs). For example, Podstawczyk and co-workers recently have chosen alginate and methylcellulose as hydrogel precursors, the latter was used as a viscosity-modifier of the former (Fig. 8a). In this study, polyacrylic acid (PAA) stabilized-magnetic nanoparticles embedded not only provided magnetic responsiveness, but also altered the physicochemical properties of polymer network as nanofillers [95]. In another study, the Nuzzo research group has optimized ionotropic hydrogels and nanocomposites for 3D printing and fabricated a magnetic field-driven actuator as a demonstration [96]. The Serra research group has applied a low intensity magnetic field to generate the anisotropic nanocomposite hydrogels [97]. As a demonstration, the actuation of a printed soft robot was controlled through on/off switching of three electromagnets placed on the left (ML), right (MR) and bottom (MB) respectively (Figs. 8b and c). The simple and biocompatible process could fabricate hydrogels driven by magnetic field, temperature and light, showing great application potential in bio-actuators.

3.6. Other hydrogel actuators by DIW

Inspired by photolithography [98–100] and ionprinting [101–103] of hydrogels, Li's group has incorporated 3D printing with

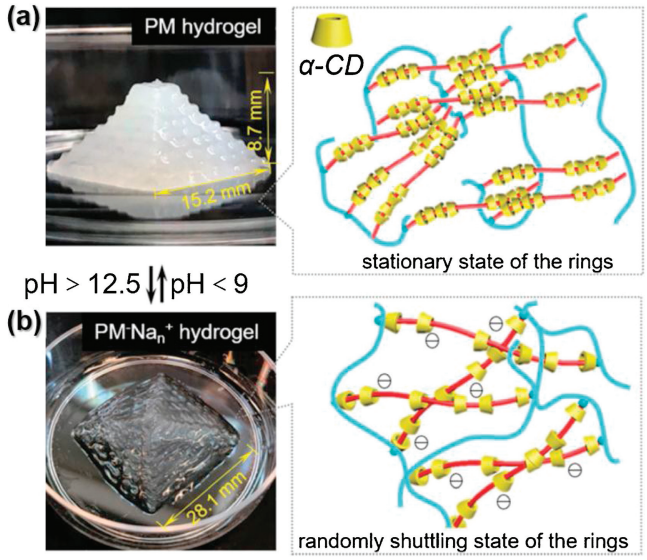

Fig. 9. pH responsive behavior of polyrotaxane monolith (PM). (a) Morphology of fabricated PM. (b) At pH 14, the pyramid (PM$^-$Na$_n^+$) deformed into a low profile expanded shape. Reproduced with permission [106]. Copyright 2018, the Royal Society of Chemistry.

versatile method called ionic crosslink lithography to introduce inhomogeneities, where in-plane and through-thickness gradient structure was formed by imposing pattern mask followed by soaking in salt solution [104]. Naficy and co-workers have developed a 3D printed multi-responsive hydrogel that deformed in response to hydration and temperature. Here, UV curable NIPAm or HEMA monomers form interpenetrating network with polyether-based polyurethane. Various molecular weight of the latter helped adjust the rheological property of inks for printing [105]. By direct ink printing and post-printing crosslinking of dimethacrylamide-poly(ethylene-glycol) and α-CD, a rapid pH/ionic strength responsive material was fabricated based on on-off switch of hydrogen bond upon pH and ionic strength variation (Fig. 9). The forming and re-forming of the hydrogen-bonding between α-CD rings could be triggered by pH and ionic strength. This kind of ring motions at molecular level would be fast compared to coil-globule transition in conventional PNIPAm-based actuator [106]. In another elegant work on DIW printing multi-responsive hydrogel, triple stimuli-responsive ABA triblock copolymer was used to build actuators responsive to pressure, temperature and UV light [107].

To have a better understanding on the development of 3D printing hydrogel actuators, Table 1 summarizes different hydrogel actuators and their properties classified by response types. It can be found that the response types of hydrogel actuators are mainly determined by the materials' physicochemical properties.

3.7. Recent developments to improve resolution or actuation time of hydrogel actuators by DIW

In extrusion-based hydrogel printing, the resolutions are typically sub-millimeter. DIW enjoys great freedom to develop functional composite at a large resolution range of filament diameter from 1 μm to 250 μm [108]. Relatively low resolution compared to light-responsive techniques hinders the improvement of actuation speed. Recently, Zhang and colleagues have proposed a method to enhance resolution *via* charge complexation of polyionic network, leading to the expulsion of water (Figs. 10a and b). This strategy, named as "shrinking printing", achieved a shrinkage of about 11% in size for hyaluronic acid methacrylate (HAMA), without the necessity of upgrading printer hardware.

Table 1
A summary for 3D printed hydrogel actuators and their properties.

Response type(s)	Printing technique	Main material(s)	Proposed application(s)	Authors	Year	Ref.
Light	MPL	PNIPAm, AuNRs	Microswimmer, artificial muscle	Möller *et al.*	2020	[41]
Light	DIW	PNIPAm, GO	Gripper	Zhang *et al.*	2019	[56]
Light	DIW	Sodium alginate, GO		Zhang *et al.*	2020	[57]
Light	DIW	Chitosan, GO	Smart curtain, remote control device	Sang *et al.*	2020	[58]
Electric-field	PμSL	PEGDA, PAA	Artificial muscle	Lee *et al.*	2018	[48]
Electric-field	DIW	Chitosan		Kaynak *et al.*	2017,2018	[62–64]
Electric-field	DIW	PAAm, silicon		McAlpine *et al.*	2018	[65]
Thermal	PμSL	PNIPAm	Gripper, microfluidic	Lee *et al.*	2018	[47]
Thermal	DIW	Agarose, laponite		Zhang *et al.*	2018	[69]
Thermal	DIW	PEG, α-CD		Ke *et al.*	2020	[72]
Thermal	DIW	P(DMMAAm-co-SA)	Gripper	Furukawa *et al.*	2019	[104]
Thermal + light	DIW	PNIPAm, laponite, CNT	Motion sensor	Guo *et al.*	2019	[68]
Thermal + pH	SLA	PNIPAm, PCEA	Gripper	Raquez *et al.*	2019	[37]
Thermal + pH	DIW	Chitosan, nZnO	Scaffold with antibacterial activity	Rivero *et al.*	2020	[113]
Water	DIW	Methylcellulose	Cell sheets	Rimondini *et al.*	2018	[73]
Water	DIW	NFC		Lewis *et al.*	2016	[74]
Water	DIW	PDMAA, NFC		Zhou *et al.*	2020	[75]
Water	DIW	Egg white, CNT	Wearable electronics	Xing *et al.*	2019	[78]
Water (humidity)	DIW	Eu^{3+} ion-coordinated zwitterionic PEI-co-PAA, PEGDA	Camouflageable actuators	Zhou *et al.*	2020	[110]
Magnetic-field	DIW	PAA, MNPs	Drug delivery systems	Podstawczyk *et al.*	2020	[79]
Magnetic-field	DIW	Alginate, MNPs		Nuzzo *et al.*	2019	[80]
Magnetic-field	DIW	PEG, MNPs	Magnetic soft robot	Serra *et al.*	2019	[81]
Ion	SLA	PEGDA, PAA	Plug-and-play part, microfluidic	Wong *et al.*	2016	[36]

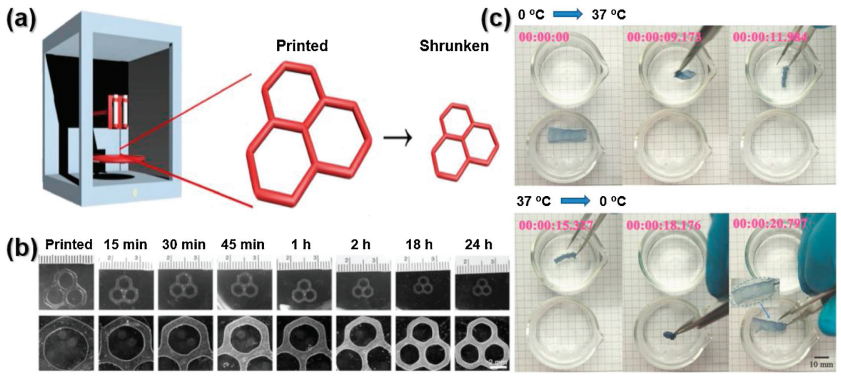

Fig. 10. (a) Schematics showing the concept of shrinking printing, where a printed hydrogel structure is post-treated to reduce its size and achieve higher resolution. (b) Photographs (upper) and micrographs (lower) showing size changes of printed hydrogels during the 24 h shrinking process. Reproduced with permission [109]. Copyright 2020, Nature Publishing Group; and (c) Shape-morphing processes of the sample prepared from combined 3D printing and electrospinning. Reproduced with permission [110]. Copyright 2018, Wiley-VCH.

Further, this shrinking process was proved to maintain cytocompatibility conditions while enhancing printing resolution [109].

In order to accelerate the response of hydrogel actuators, the Agarwal research group has constructed a series of porous hydrogel actuators by creatively combining electrospinning and 3D printing [110]. Time needed for thermal actuation from 0 °C to 37 °C is 2.8 s and reversely from 37 °C to 0 °C is 2.6 s (Fig. 10c). The actuation time was slightly longer than the pure electrospinning PNIPAm actuators in their previous study (< 1 s) [111], which might be ascribed to the shape difference. High porosity of electrospinning mesostructured substrates enhanced mass transporting and rendered the actuators fast response. The combined electrospinning and 3D printing method provided a promising framework to generate fast responsive soft actuators.

3.8. Recent developments to improve printability of hydrogel actuators by DIW

Viscosity is one of the most important properties of suitable inks. The selection of hydrogels for printing is limited to fulfill the specific viscosity of inks. As for light-curing techniques such as SLA a lower viscosity is preferred [112]. While for DIW, it requires a relatively high viscosity (10^3–10^6 mPa·s) and shear thinning behavior (a decrease of viscosity with an increase of shear forces inside the nozzle) [113]. To extend the scope of available hydrogel inks, Yum *et al.* presented a generalizable method to print low viscosity precursor solutions using gel-phase fugitive carrier with shear-thinning properties. The shear-thinning behavior of the carrier rendered the ink 3D printable, whereas the thermally reversible gel-to-fluid transition allowed for the complete removal of the carrier from printed structures. Various precursor solutions such as NIPAm and PEGDA solutions were employed to demonstrated the feasibility of the method [114].

To improve the printability of inks, various rheology modifiers (Pluronic F-127, nano clay, *etc.*) have been used. Recently, the Qu research group has presented the feasibility of using Carbomer as the rheology modifier, where only a low dosage (~0.5%) was required to achieve the appropriate rheology [115]. Huang and coworkers have added the Laponite nanoclay to NIPAAm hydrogels. The fabricated PNIPAm-Laponite and PNIPAm-Laponite-GO nanocomposite hydrogels showed predictable pattern deformation due to their different shrinking ratios and mechanical properties [116].

Non-homogeneous thickening modifiers such as nanoclay and silica particles, although able to render the ink desired rheological property, can impair the softness, transparency and responsiveness of hydrogel actuators. Thus, a homogeneous alginate-based modifier was chosen by Ho and colleagues. It percolated ionically to form hydrophilic polymer network and modified the rheology of inks without harming the valuable properties of pristine hydrogels (Fig. 11). Interestingly, the introduced ionic crosslinking not only enabled the rheological turning but also contributed to enhancement of mechanical toughness. Based on this method, representative prototypes were made including an artificial tentacle, a robotic heart and an artificial tendril [117].

The applications of hydrogel inks in structures with internal gaps or suspended beam structures were restricted because of the low viscosity. To address this problem, Onoe and co-workers have introduced viscous carboxymethyl cellulose solution (CMCaq) as a supporting viscous liquid during printing. 4D structures with internal gaps were fabricated by printing a mixture of NIPAm-based and AAm-based ink in CMCaq [118]. For more hints on adjusting the printability, the readers are referred to a recent review highlighting the chemical and physical factors governing the printability of bioinks [119].

4. Applications and optimization of 3D printed hydrogel actuators

4.1. Applications

As one of the most common applications, hydrogel grippers are generally realized from bilayer structures. For example, Furukawa and co-workers have realized an underwater soft gripper (Fig. 12a). The concept was demonstrated with bilayer composed of poly(*N*, *N*′-dimethyl acrylamide-*co*-stearyl acrylate) (P(DMAAm-*co*-SA))-based hydrogels with different concentration of the crystalline monomer SA in the shape-memory-hydrogel. Different SA concentration in the gel contributed to the mechanical and swelling anisotropy, resulting in the actuation movements [120].

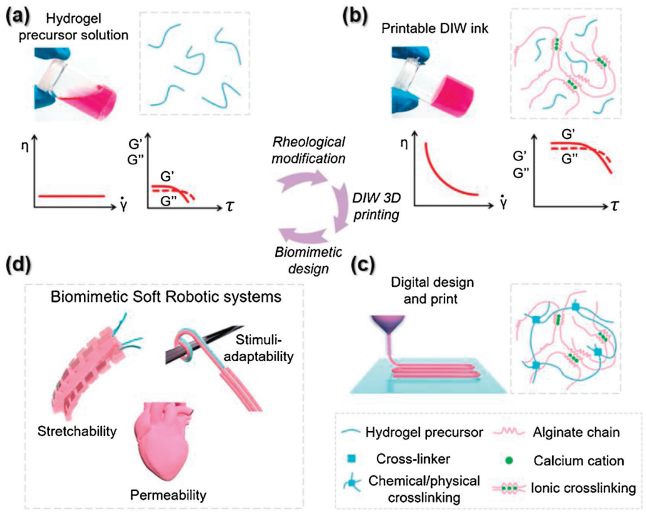

Fig. 11. (a) Schematic illustration of DIW 3D printing with rheological modification. (a) Hydrogel precursor solution photo (AAm as an example here) with the composition diagram and the typical water-like rheological behavior. (b) Printable DIW ink photo with the composition diagram and typical gel-like rheological behavior after rheological modification. (c) Digital design and print of DIW ink (schematic) and the composition diagram after hydrogel curing. (d) Biomimetic soft robotic system (schematic) including an artificial tentacle, a bioengineered robotic heart, and an artificial tendril. Reproduced with permission [117]. Copyright 2019, American Chemical Society.

Among the interesting potential applications of 3D printed hydrogel actuators, a smart valve was devised by the Spinks research group to control water flow based on 3D printed alginate/PNIPAm ICE hydrogels. Here, PNIPAm acted as both the toughening agent and the actuation provider through its characteristic reversible volume transition at T_c [121].

Thin elastic objects undergo out-of-plane buckling are common in biological morphogenesis. Given their high biocompatibility and easy fabrication, 3D printed stimuli-responsive hydrogels have been considered as promising candidates in this field. For example, self-holding hollow tubes mimicking blood vessels based on 3D bioprinting alginate and hyaluronic acid have been reported by the Ionov research group [122]. Inspiring from plant leaves and flowers, complex shape-morphing can be realized by femtosecond laser direct writing of stimuli-responsive hydrogels [123–125].

Inspired by plants and marine animals that change shapes or colors on stimuli, a biomimetic ink was recently developed that can be 3D printed to endow the actuators with shape, luminescence and opacity changes in response to humidity or (de) hydration (Fig. 12b) [126]. Full color luminescence herein ascribed to fluorophore-PEI-*co*-PAA copolymer and fluorophore-lanthanide complexes. Whereas the opacity tunability was provided by reversible phase separation of zwitterionic polymers. The fabricated stimuli-responsive hydrogel was a sound demonstration of a camouflageable soft actuator.

Scientists have also integrated 3D printed hydrogels with other materials to achieve certain properties. For example, Suo and colleagues have developed a method for 3D printing and direct integration of PAAm hydrogel and PDMS elastomer at sub-millimeter resolution. Compared to traditional methods which usually require casting or other techniques, this approach provided a simple pathway to fabricate hydrogels and dielectric elastomers in an integrated manner [127].

High biocompatibility makes 3D printed hydrogels sound choices for biomedicine and tissue engineering. Cohn *et al.* have demonstrated the potential application of 3D printed stimuli-responsive hydrogel in medical devices by using SLA technique. Methacrylated poly(ethylene oxide)-poly(propylene oxide)-poly (ethylene oxide) triblocks were chosen as the basic blocks of the reverse thermo-responsive and pH-sensitive hydrogel [128]. In another study, chitosan-based thermal and pH responsive hydrogels were fabricated by means of DIW, with the antibacterial activity of zinc oxide nanoparticles [129].

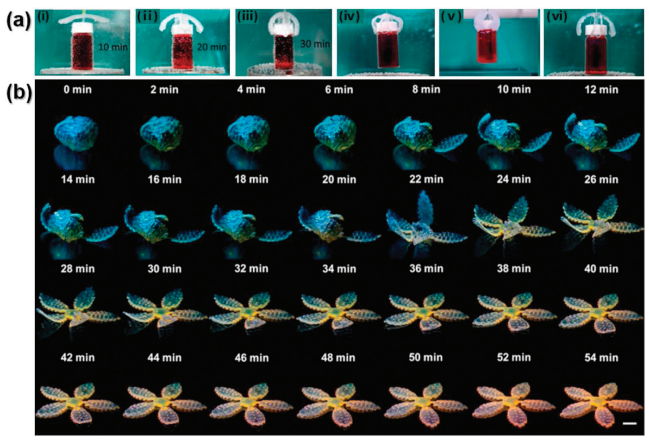

Fig. 12. (a) 3D macroscopic gripper at different bending positions. Reproduced with permission [120]. Copyright 2019, Wiley-VCH. (b) Four-dimensional printing of simultaneous full-color luminescence tuning and shape morphing architectures. Reproduced with permission [126]. Copyright 2020, American Chemical Society.

4.2. Toughness of hydrogel actuators

Traditional pure hydrogel-based actuators show limited stiffness and toughness, which hinders their constant usage. Also, mechanical properties are lowered by manufacturing process of extrusion-based DIW that introduces mechanical anisotropy in product [130]. One solution to this problem is to integrate with other materials by multi-material 3D printing. Qi and colleagues have designed shape memory polymer (SMP)-hydrogel components where hydrogel provided driving force for the shape change, and SMP regulated the time of such shape change. Further, SMP yielded the structure stiffness that was much higher than pure gel [131].

There is usually a trade-off between high mechanical properties and fast actuating speed in hydrogel devices. Wu and co-workers have incorporated highly viscoelastic P(AAc-*co*-AAm) and P(AAc-*co*-NIPAm) solutions or their mixtures into $FeCl_3$ solution, where robust carboxyl-Fe^{3+} coordination complexes were formed, affording robust mechanical properties [132]. Furthermore, Wu and his colleagues have also conducted beautiful works on 3D printing tough polyion complex hydrogels (Fig. 13a) [133]. On one hand, being viscous solution in concentrated saline solution, polyion complex underwent sol-gel transition when extruded out into water, rendering fine printability. On the other hand, the breaking and re-forming of ion bonds dissipated energy and provided high toughness for soft actuators. This method provided a versatile platform to 3D print hydrogel actuators based on tough polyion complex. In another research on toughening hydrogel by ions, the fracture energy of hydrogels increased significantly by introducing reversible Ca^{2+} crosslinking and long chains into alginate [134].

Double-network (DN) hydrogels, which consists of polymer networks with contrasting physical properties, showed extremely toughness, because the brittle first network ruptured and dissipated a large amount of energy before the whole gel fractured [135,136]. Based on DN concept, Zhong and co-workers have developed a kind of tough 3D printable hydrogel ink consisting of a physically crosslinked graphene oxide (GO) network and a chemically crosslinked polyacrylic acid (PAA) network. The hydrogel achieved a toughness of 9.73 MJ/m^3 and an elongation ratio of 2500% [75]. In another case employing the DN strategy, the Amstad research group has introduced polyelectrolyte microgels into acrylamide monomer, the latter could be converted into a percolating network, enhancing the mechanical properties of the pristine hydrogel (Fig. 13b) [137]. This work elegantly separated the fabrication of microgels and their annealing, thus combined the advantages of jammed granular solutions such as injectability and printability with the excellent toughness of DN hydrogels. With another toughening concept, scientists have designed self-growing hydrogels that gain strength in usage by training [138,139], which provide promising materials for actuator applications.

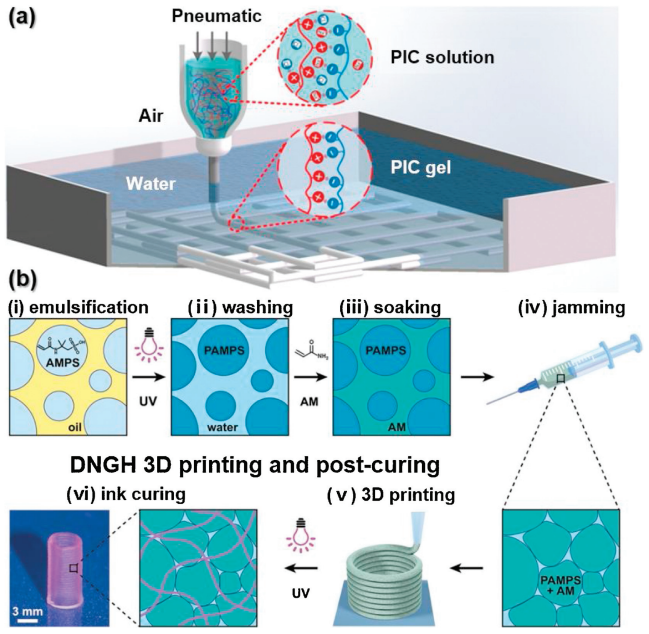

Fig. 13. (a) Schematic of 3D printing system and sol–gel transition mechanism. The viscous PIC solution was loaded into a syringe and extruded pneumatically into deionized water *via* a customized 3D printing platform. In water, the viscous PIC solution rapidly gelated into a tough solid gel by dialyzing out the salt and counterions of PIC. Reproduced with permission [133]. Copyright 2016, American Chemical Society. (b) Schematic representation of microgel fabrication employing DN concept. Reproduced with permission [137]. Copyright 2020, Wiley-VCH.

4.3. Finite element analysis (FEA) and closed loop design of hydrogel actuators

The physical phenomena of actuation are complicated. For instance, motions of hydrogel with irregular shapes are nonlinear, and the effects of environmental stimuli and material composition add complexities. Therefore, controllable actuation movement and output force are desirable [140]. And there is an increasing demand of developing theoretical models to help understand the interplay of various stimuli parameters and evaluate actuator's performance [131]. Besides, finite element analysis can also be employed to predict bioprintability of inks [141].

With a combined FEA and experiment method, Gracias and co-workers have interpreted the design principle of strategic placement of 3D printed segment of dual materials consisting of swelling and non-swelling parts to achieve various functions or movements [142]. Here, parameters in the constitutive model of hydrogels were calibrated with two parts: a *quasi*-incompressible neo-Hookean model for the entropy elasticity of polymer network chain, and the Flory-Huggins model for the mixing energy between polymer network and solvent. The calibrated finite element model successfully reproduced the actuation of hydrogels accurately (Fig. 14a).

Model-based simulation enables design and fabrication of complex shape-morphing structures *via* accurately predicting 3D morphologies [108]. Both analytical and finite element model were employed to account for large-range twisting and contractile motions induced by pressurization [143]. The calculated soft actuator shapes and strain distribution were comparable to experiment results (Fig. 14b). Furthermore, by integrating 3D printed soft actuators and sensors with FEA and (or) data-driven machine learning, the concept of "closed loop 3D printed soft robot" was demonstrated where the robots can respond to environmental interactions and stimuli without the necessity of accepting commands from outside users [144].

5. Perspectives

Despite the tremendous progress and more attention of this area, it still has a long way to go for the application of 3D printed hydrogel actuators. For example, nowadays hydrogel actuators undergo limited movements and output force. Therefore, it is vital to improve the energy conversion efficiency and energy density.

As for the material aspect, novel biomimetic materials will provide new possibilities into this field. With the mild reaction conditions and effective control of formation of hydrogels from

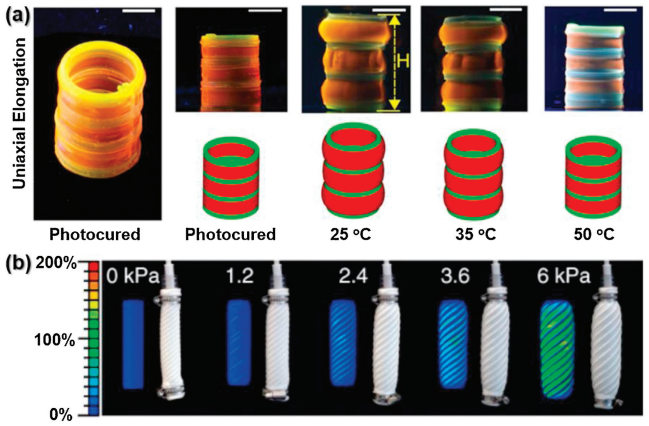

Fig. 14. (a) Optical and FEA snapshots of shape change of tubes at different temperatures. Scale bar: 1 cm. Reproduced with permission [142]. Copyright 2019, American Chemical Society. (b) Calculated first principal strain distribution and soft actuator shapes compared to experimental photographs. Reproduced with permission [143]. Copyright 2018, Nature Publishing Groups.

time and space, state-of-the-art photopolymerizable materials may be suitable choices for light-curing printing in tissue engineering [145]. Self-healing or self-recoverable properties of hydrogels [146–148], ascribed from dynamic bonds in molecular structures such as hydrogen bonds and ionic bonds, can add to the stabilization of the structures. Meanwhile, compared to traditional free radical polymerization, integration with controlled reactions such as reversible addition-fragmentation chain-transfer (RAFT) [149] and click reaction [150] may lead to well-defined microstructures and thus precise control of actuation. In addition, the continuously developing elastic theory [151] of hydrogels may provide new hints for hydrogel design as structural materials.

Further improvement of printing resolution may empower development of micro-machine technology. The combined resorbable electrospun nanofibers [152] and 3D printing may broaden the application of hydrogel actuators in recyclable tissue engineering. Optimization of actuator structures and improvement of material properties will broaden the application of 3D printed stimuli-responsive hydrogels. With the development of quantum computing and parallel computing, IT technologies will pose an increasing impact on this field. A combination of analytical method, finite element analysis and artificial intelligence may deepen our understanding of the energy transition process in actuation.

6. Conclusions

In summary, firstly a glance was taken on the important aspects of 3D printing hydrogel actuators, namely material, printing and actuation. Then, recent progress concerning 3D printed hydrogel actuators was picked up based on the mechanisms of printing and actuation. After that, an introduction of applications was presented followed by discussions of printing resolution, toughness and finite element analysis method. Finally, the review was concluded with a perspective on the area. Successful fabrication of 3D printed hydrogel actuators calls for careful design and trial-and-error efforts concerning materials, printing and actuation process. Thus interdisciplinary collaboration are desired. Many high-impact works of 3D printed hydrogel actuators have been reported with various advantages over traditional ones. Despite the challenges yet overcome, 3D printed hydrogel actuators will attract more and more attention from different societies, such as 3D printing, hydrogels, actuators, polymers.

Declaration of competing interest

The authors declared that they have no conflicts of interest to this work. We declare that we do not have any commercial or associative interest that represents a conflict of interest in connection with the work submitted.

Acknowledgements

This work is supported by Changzhou Sci&Tech Program (Nos. CZ20200009, CJ20190017, CE20200089), Qinglan Project of Jiangsu (No. Su 2018-12), Young Fund, Doctoral Fund and Research Team of Changzhou Institute of Industry Technology (Nos. QN201813101011, BS202013101007, ZD201813101003), and Natural Science Foundation of Jiangsu Province (No. BK20180770).

References

[1] R.V. Ham, T.G. Sugar, B. Vanderborght, K.W. Hollander, D. Lefeber, IEEE Robot. Autom. Lett. 16 (2009) 81–94.
[2] L. Liu, H. Bakhshi, S. Jiang, H. Schmalz, S. Agarwal, Macromol. Rapid Commun. 39 (2018) 1800082.
[3] S. Agarwal, S. Jiang, Y. Chen, Macromol. Mater. Eng. 304 (2019) 1800548.
[4] L. Liu, W. Xu, Y. Ding, et al., Compos. Commun. 22 (2020) 100506.
[5] H. Qian, J. Wang, L. Yan, J. Bioresour. Bioprod. 5 (2020) 204–210.
[6] S. Jiang, G. Duan, U. Kuhn, et al., Angew. Chem. Int. Ed. 56 (2017) 3285–3288.
[7] E.M. Ahmed, J. Adv. Res. 6 (2015) 105–121.
[8] C. Zheng, S. Zhu, Y. Lu, et al., J. For. Eng. 5 (2020) 93–100.
[9] Y. Wang, S. Zhang, J. Wang, Chin. Chem. Lett. 32 (2021) 1603–1614.
[10] H. Zhang, J. Jiang, J. Li, et al., J. For. Eng. 5 (2020) 76–81.
[11] B. Sui, Y. Li, B. Yang, Chin. Chem. Lett. 31 (2020) 1443–1447.
[12] Z. Yuan, H. Lin, X. Qian, J. Shen, J. Bioresour. Bioprod. 4 (2019) 214–221.
[13] Z. Xia, J. Li, J. Zhang, et al., J. Bioresour. Bioprod. 5 (2020) 79–95.
[14] X. Han, G. Xiao, Y. Wang, et al., J. Mater. Chem. A 8 (2020) 23059–23095.
[15] K. Huang, G. Liu, Z. Gu, J. Wu, Chin. Chem. Lett. 31 (2020) 3190–3194.
[16] K. Huang, J. Wu, Z. Gu, ACS Appl. Mater. Interfaces 11 (2019) 2908–2916.
[17] G. Liu, Z. Bao, J. Wu, Chin. Chem. Lett. 31 (2020) 1817–1821.
[18] X. Deng, B. Huang, Q. Wang, et al., ACS Sustain. Chem. Eng. 9 (2021) 3070–3082.
[19] W. Liu, C. Si, H. Du, et al., J. For. Eng. 4 (2019) 11–19.
[20] G. He, X. Yan, Z. Miao, et al., Chin. Chem. Lett. 31 (2020) 1807–1811.
[21] H. Wu, W. Li, M. Zhao, et al., J. For. Eng. 5 (2020) 11–17.
[22] G. Liu, Q. Yuan, G. Hollett, et al., Polym. Chem. 9 (2018) 3436–3449.
[23] X. Li, M. Fu, J. Wu, et al., Acta Biomater. 51 (2017) 294–303.
[24] T. Yi, S. Huang, G. Liu, et al., ACS Appl. Bio Mater. 1 (2018) 193–209.
[25] J. Wu, D. Wu, M.A. Mutschler, C.C. Chu, Adv. Funct. Mater. 22 (2012) 3815–3823.
[26] C. Liu, W. Zheng, R. Xie, et al., Chin. Chem. Lett. 30 (2019) 457–460.
[27] D. Zhang, J. Cai, W. Xu, et al., J. For. Eng. 4 (2019) 92–98.
[28] L. Ionov, Mater. Today 17 (2014) 494–503.
[29] Q. Li, C. Liu, J. Wen, et al., Chin. Chem. Lett. 28 (2017) 1857–1874.
[30] Z. Jiang, M.L. Tan, M. Taheri, et al., Angew. Chem. Int. Ed. 59 (2020) 7049–7056.
[31] O. Werzer, S. Tumphart, R. Keimel, P. Christian, A.M. Coclite, Soft Matter 15 (2019) 1853–1859.
[32] S. Jiang, N. Helfricht, G. Papastavrou, A. Greiner, S. Agarwal, Macromol. Rapid Commun. 39 (2018) 1700838.
[33] L. Zhao, G. Duan, G. Zhang, et al., Nanomaterials 10 (2020) 150.
[34] K. Molnar, A. Jedlovszky-Hajdu, M. Zrinyi, S. Jiang, S. Agarwal, Macromol. Rapid Commun. 38 (2017) 1700147.
[35] A.M. Shumatbaeva, J.E. Morozova, V.V. Syakaev, et al., Colloids Surf. A 611 (2020) 125814.
[36] G. Sharifzadeh, H. Hosseinkhani, Adv. Healthc. Mater. 6 (2017) 1700801.
[37] J.H. Ha, H.H. Shin, H.W. Choi, et al., Lab Chip 20 (2020) 3354–3364.
[38] S. Liu, H. Yang, L. Sui, S. Jiang, H. Hou, Energy Technol. 8 (2020) 2000397.
[39] A.C. Manjua, V.D. Alves, J.G. Crespo, C.A.M. Portugal, ACS Appl. Mater. Interfaces 11 (2019) 21239–21249.
[40] X. Peng, T. Liu, C. Jiao, et al., J. Mater. Chem. B 5 (2017) 7997–8003.
[41] H. Qin, T. Zhang, N. Li, H.-P. Cong, S.H. Yu, Nat. Commun. 10 (2019) 2202.
[42] X. Zhao, L. Zhao, Q. Xiao, H. Xiong, Chin. Chem. Lett. 32 (2021) 1363–1366.
[43] X. Peng, T. Liu, Q. Zhang, et al., Adv. Funct. Mater. 27 (2017) 1701962.
[44] H. Wen, J. Li, G.F. Payne, et al., Biofabrication 12 (2020) 035007.
[45] R.L. Truby, J.A. Lewis, Nature 540 (2016) 371–378.
[46] M. Tyagi, G.M. Spinks, E.W.H. Jager, Soft Robot. (2020) 19–27.
[47] X. Peng, H. Wang, J. Polym. Sci. Part B: Polym. Phys. 56 (2018) 1314–1324.
[48] X. Le, W. Lu, J. Zhang, T. Chen, Adv. Sci. 6 (2019) 1801584.
[49] A. Zolfagharian, A.Z. Kouzani, S.Y. Khoo, et al., Sens. Actuator. A 250 (2016) 258–272.
[50] M. Champeau, D.A. Heinze, T.N. Viana, et al., Adv. Funct. Mater. 30 (2020) 1910606.

[51] A. Ehrenhofer, S. Binder, G. Gerlach, T. Wallmersperger, Adv. Eng. Mater. 22 (2020) 2000004.
[52] Z. Zhu, D.W.H. Ng, H.S. Park, M.C. McAlpine, Nat. Rev. Mater. 6 (2020) 27–47.
[53] T.M. Valentin, E.M. DuBois, C.E. Machnicki, et al., Polym. Chem. 10 (2019) 2015–2028.
[54] J. Odent, S. Vanderstappen, A. Toncheva, et al., J. Mater. Chem. A 7 (2019) 15395–15403.
[55] X. Sun, P. Tyagi, S. Agate, et al., Carbohydr. Polym. 234 (2020) 115898.
[56] A.K. Mishra, T.J. Wallin, W. Pan, et al., Sci. Robot. 5 (2020) eaaz3918.
[57] C. Garcia, A. Gallardo, D. López, et al., ACS Appl. Bio Mater. 1 (2018) 1337–1347.
[58] M.R. Lee, I.Y. Phang, Y. Cui, Y.H. Lee, X.Y. Ling, Small 11 (2015) 740–748.
[59] A. Nishiguchi, H. Zhang, S. Schweizerhof, et al., ACS Appl. Mater. Interfaces 12 (2020) 12176–12185.
[60] C. Lv, X.C. Sun, H. Xia, et al., Sens. Actuator. B 259 (2018) 736–744.
[61] E. Scarpa, E.D. Lemma, R. Fiammengo, et al., Sens. Actuator. B 279 (2019) 418–426.
[62] X.H. Qin, X. Wang, M. Rottmar, B.J. Nelson, K. Maniura-Weber, Adv. Mater. 30 (2018) 1705564.
[63] Z. Xiong, M.L. Zheng, X.Z. Dong, et al., Soft Matter 7 (2011) 10353–10359.
[64] D. Han, Z. Lu, S.A. Chester, H. Lee, Sci. Robot. 8 (2018) 1963.
[65] D. Han, C. Farino, C. Yang, et al., ACS Appl. Mater. Interfaces 10 (2018) 17512–17518.
[66] L. Huang, R. Jiang, J. Wu, et al., Adv. Mater. 29 (2017) 1605390.
[67] L. Larush, I. Kaner, A. Fluksman, et al., J. 3D Print. Med. 1 (2017) 219–229.
[68] D. Han, C. Yang, N.X. Fang, H. Lee, Addit. Manuf. 27 (2019) 606–615.
[69] M. Zhang, A. Vora, W. Han, et al., Macromolecules 48 (2015) 6482–6488.
[70] M. Nadgorny, Z. Xiao, C. Chen, L.A. Connal, ACS Appl. Mater. Interfaces 8 (2016) 28946–28954.
[71] E. Zhang, T. Wang, W. Hong, et al., J. Mater. Chem. A 2 (2014) 15633–15639.
[72] Q. Zhao, Y. Liang, L. Ren, et al., J. Mech. Behav. Biomed. Mater. 78 (2018) 395–403.
[73] L. Zhang, X. Zhang, L. Li, et al., Macromol. Mater. Eng. 305 (2020) 1900718.
[74] M. Zhang, Y. Wang, M. Jian, et al., Adv. Sci. 7 (2020) 1903048.
[75] Y. Wang, Q. Chang, R. Zhan, et al., J. Mater. Chem. A 7 (2019) 24814–24829.
[76] S.H. Hsiao, S.H. Hsu, ACS Appl. Mater. Interfaces 10 (2018) 29273–29287.
[77] H.J. Kwon, Y. Osada, J.P. Gong, Polym. J. 38 (2006) 1211–1219.
[78] A. Zolfagharian, A.Z. Kouzani, S.Y. Khoo, B. Nasri-Nasrabadi, A. Kaynak, Sens. Actuator. A 265 (2017) 94–101.
[79] A. Zolfagharian, A. Kaynak, S.Y. Khoo, A.Z. Kouzani, 3D Print. Add. Manuf. 5 (2018) 138–150.
[80] A. Zolfagharian, A.Z. Kouzani, S.Y. Khoo, A. Noshadi, A. Kaynak, Smart Mater. Str. 27 (2018) 045019.
[81] G. Haghiashtiani, E. Habtour, S.H. Park, F. Gardea, M.C. McAlpine, Extreme Mech. Lett. 21 (2018) 1–8.
[82] Y. Guo, J.A. Belgodere, Y. Ma, J.P. Jung, B. Bharti, Macromol. Rapid Commun. 40 (2019) 1900191.
[83] H. Warren, D.J. Shepherd, M. in het Panhuis, D.L. Officer, G.M. Spinks, Sens. Actuators A 301 (2020) 111784.
[84] Z. Deng, T. Hu, Q. Lei, et al., ACS Appl. Mater. Interfaces 11 (2019) 6796–6808.
[85] J. Guo, R. Zhang, L. Zhang, X. Cao, ACS Macro Lett. 7 (2018) 442–446.
[86] Y. Okumura, K. Ito, Adv. Mater. 13 (2001) 485–487.
[87] Q. Lin, X. Hou, C. Ke, Angew. Chem. Int. Ed. 56 (2017) 4452–4457.
[88] Q. Lin, M. Tang, C. Ke, Polym. Chem. 11 (2020) 304–308.
[89] A. Cochis, L. Bonetti, R. Sorrentino, et al., Materials 11 (2018) 579.
[90] A.S. Gladman, E.A. Matsumoto, R.G. Nuzzo, L. Mahadevan, J.A. Lewis, Nat. Mat. 15 (2016) 413–418.
[91] S. Zhou, Q. Zhou, C. Lu, Z. Zhang, L. Ren, e-Polym. 20 (2020) 273–281.
[92] L.H. Fu, C. Qi, M.G. Ma, P. Wan, J. Mater. Chem. B 7 (2019) 1541–1562.
[93] M.C. Mulakkal, R.S. Trask, V.P. Ting, A.M. Seddon, Mater. Des. 160 (2018) 108–118.
[94] Q. Chang, M.A. Darabi, Y. Liu, et al., J. Mater. Chem. A 7 (2019) 24626–24640.
[95] D. Podstawczyk, M. Nizioł, P. Szymczyk, P. Wiśniewski, A. Guiseppi-Elie, Addit. Manuf. 34 (2020)101275.
[96] J.M. McCracken, B.M. Rauzan, J.C.E. Kjellman, et al., Adv. Funct. Mater. 29 (2019)1806723.
[97] R. Tognato, A.R. Armiento, V. Bonfrate, et al., Adv. Funct. Mater. 29 (2019) 1804647.
[98] R. Takahashi, Z.L. Wu, M. Arifuzzaman, et al., Nat. Commun. 5 (2014) 4490.
[99] Z.J. Wang, C.N. Zhu, W. Hong, Z.L. Wu, Q. Zheng, Sci. Adv. 3 (2017) e1700348.
[100] Z.J. Wang, W. Hong, Z.L. Wu, Q. Zheng, Angew. Chem. Int. Ed. 56 (2017) 15974–15978.
[101] B.P. Lee, S. Konst, Adv. Mater. 26 (2014) 3415–3419.
[102] E. Palleau, D. Morales, M.D. Dickey, O.D. Velev, Nat. Commun. 4 (2013) 2257.
[103] X. Peng, Y. Li, Q. Zhang, et al., Adv. Funct. Mater. 26 (2016) 4491–4500.
[104] X. Li, D. Xu, H. Wang, et al., Macromol. Rapid Commun. 41 (2020) 2000127.
[105] S. Naficy, R. Gately, R. Gorkin III, H. Xin, G.M. Spinks, Macromol. Mater. Eng. 302 (2017)1600212.
[106] Q. Lin, L. Li, M. Tang, X. Hou, C. Ke, J. Mater. Chem. C 6 (2018) 11956–11960.
[107] D.G. Karis, R.J. Ono, M. Zhang, et al., Polym. Chem. 8 (2017) 4199–4206.
[108] Y. Kim, H. Yuk, R. Zhao, S.A. Chester, X. Zhao, Nature 558 (2018) 274–279.
[109] J. Gong, C.C.L. Schuurmans, A.M.V. Genderen, et al., Nat. Commun. 11 (2020) 1267.
[110] T. Chen, H. Bakhshi, L. Liu, J. Ji, S. Agarwal, Adv. Funct. Mater. 28 (2018) 1800514.
[111] S. Jiang, F. Liu, A. Lerch, L. Ionov, S. Agarwal, Adv. Mater. 27 (2015) 4865–4870.
[112] R.D. Farahani, M. Dubé, D. Therriault, Adv. Mater. 28 (2016) 5794–5821.
[113] N.W.S. Pinargote, A. Smirnov, N. Peretyagin, A. Seleznev, P. Peretyagin, Nanomaterials 10 (2020) 1300.
[114] H. Arslan, A. Nojoomi, J. Jeon, K. Yum, Adv. Sci. 6 (2019) 1800703.
[115] Z. Chen, D. Zhao, B. Liu, et al., Adv. Funct. Mater. 29 (2019) 1900971.
[116] Y. Jin, Y. Shen, J. Yin, J. Qian, Y. Huang, ACS Appl. Mater. Interfaces 10 (2018) 10461–10470.
[117] Y. Cheng, K.H. Chan, X.Q. Wang, et al., ACS Nano 13 (2019) 13176–13184.
[118] T. Uchida, H. Onoe, Micromachines 10 (2019) 433.
[119] S.C. Lee, G. Gillispie, P. Prim, S.J. Lee, Chem. Rev. 120 (2020) 10834–10886.
[120] M.D.N.I. Shiblee, K. Ahmed, M. Kawakami, H. Furukawa, Adv. Mater. Technol. 4 (2019) 1900071.
[121] S.E. Bakarich, R. Gorkin III, M.I.H. Panhuis, G.M. Spinks, Macromol. Rapid Commun. 36 (2015) 1211–1217.
[122] A. Kirillova, R. Maxson, G. Stoychev, C.T. Gomillion, L. Ionov, Adv. Mater. 29 (2017) 1703443.
[123] Y. Hu, Z. Wang, D. Jin, et al., Adv. Funct. Mater. 30 (2020) 1907377.
[124] S.-J. Jeon, A.W. Hauser, R.C. Hayward, Acc. Chem. Res. 50 (2017) 161–169.
[125] H. Kim, S.K. Ahn, D.M. Mackie, et al., Mater. Today 41 (2020) 243–269.
[126] Y. Yao, C. Yin, S. Hong, et al., Chem. Mater. 32 (2020) 8868–8876.
[127] K. Tian, J. Bae, S.E. Bakarich, et al., Adv. Mater. 29 (2017) 1604827.
[128] S. Dutta, D. Cohn, J. Mater. Chem. B 5 (2017) 9514–9521.
[129] S. Ramesh, V. Kovelakuntla, A.S. Meyer, I.V. Rivero, Bioprinting (2020) e00106.
[130] N.S. Hmeidat, R.C. Pack, S.J. Talley, R.B. Moore, B.G. Compton, Addit. Manuf. 34 (2020) 101385.
[131] Y. Mao, Z. Ding, C. Yuan, et al., Sci. Robot. 6 (2016) 24761.
[132] S.Y. Zheng, Y. Shen, F. Zhu, et al., Adv. Funct. Mater. 28 (2018) 1803366.
[133] F. Zhu, L. Cheng, J. Yin, et al., ACS Appl. Mater. Interfaces 8 (2016) 31304–31310.
[134] S. Hong, D. Sycks, H.F. Chan, et al., Adv. Mater. 27 (2015) 4035–4040.
[135] J.P. Gong, Soft Matter 6 (2010) 2583–2590.
[136] J.P. Gong, Y. Katsuyama, T. Kurokawa, Y. Osada, Adv. Mater. 15 (2003) 1155–1158.
[137] M. Hirsch, A. Charlet, E. Amstad, Adv. Funct. Mater. 31 (2020) 2005929.
[138] T. Matsuda, R. Kawakami, R. Namba, T. Nakajima, J.P. Gong, Science 363 (2019) 504.
[139] S. Lin, J. Liu, X. Liu, X. Zhao, Proc. Natl. Acad. Sci 116 (2019) 10244.
[140] J. Yin, D. Zhang, Z. Xu, et al., ACS Appl. Mater. Interfaces 12 (2020) 49042–49049.
[141] J. Göhl, K. Markstedt, A. Mark, et al., Biofabrication 10 (2018) 034105.
[142] J. Liu, O. Erol, A. Pantula, et al., ACS Appl. Mater. Interfaces 11 (2019) 8492–8498.
[143] M. Schaffner, J.A. Faber, L. Pianegonda, et al., Nat. Commun. 9 (2018) 878.
[144] A. Zolfagharian, A. Kaynak, A. Kouzani, Mater. Des. 188 (2020) 108411.
[145] A. Sun, X. He, X. Ji, et al., Chin. Chem. Lett. 32 (2021) 2117–2126.
[146] Y. Li, X. Wang, Y. Wei, L. Tao, Chin. Chem. Lett. 28 (2017) 2053–2057.
[147] P. Pan, X. Chen, H. Xing, et al., Chin. Chem. Lett. 32 (2021) 2159–2163.
[148] H. Xu, X.M. Xie, Chin. Chem. Lett. 32 (2021) 521–524.
[149] C. Xian, Q. Yuan, Z. Bao, G. Liu, J. Wu, Chin. Chem. Lett. 31 (2020) 19–27.
[150] A.K. Zhang, J. Ling, K. Li, et al., J. Polym. Sci. Part B: Polym. Phys. 54 (2016) 1227–1236.
[151] Y. Yoshikawa, N. Sakumichi, U.I. Chung, T. Sakai, Phys. Rev. X 11 (2021) 011045.
[152] T. Wu, M. Ding, C. Shi, et al., Chin. Chem. Lett. 31 (2020) 617–625.